

## **Electronic Supplementary Information (ESI) for:**

### **Highly Flexible Chemical Sensors Based on Polymer Nanofiber Field-Effect Transistors**

O Young Kweon,<sup>a</sup> Moo Yeol Lee,<sup>a</sup> Teahoon Park,<sup>b</sup> Hanbit Jang,<sup>a</sup> Ayoung Jeong,<sup>a</sup> Moon-Kwang Um<sup>\*b</sup> and Joon Hak Oh<sup>\*c</sup>

<sup>a</sup>Department of Chemical Engineering, Pohang University of Science and Technology (POSTECH), Pohang, 37673, Republic of Korea.

<sup>b</sup>Carbon Composites Department, Composites Research Division, Korea Institute of Materials Science (KIMS), Changwon, 51508, Republic of Korea.

<sup>c</sup>School of Chemical and Biological Engineering, Seoul National University, Seoul 08826, Republic of Korea.

\*E-mail: [joonhoh@snu.ac.kr](mailto:joonhoh@snu.ac.kr), [umk1693@kims.re.kr](mailto:umk1693@kims.re.kr)

## **Table of Contents**

### **Supplementary Section**

Procedures for self-assembled monolayer (Section S1) ----- S3

### **Supplementary Figures**

Transfer characteristics of PQT-12/C[8]A OFETs (Fig. S1) ----- S4

2D-GIXD images of PQT-12 based NFs (Fig. S2) ----- S5

The normalized  $I_D/I_{BASE}$  of a PQT-12/C[8]A OFET sensor (Fig. S3) ----- S6

The relative response of a PQT-12 based OFET sensor in harsh conditions (Fig. S4) ----- S7

Electrical characteristics of PQT-12 NF based OFET (Fig. S5) ----- S8

### **Supplementary Tables**

Summary of the electrical characteristics of PQT-12/C[8]A OFETs (Table S1) -----

S9

Primary lamellar spacing values of the PQT-12 based NFs (Table S2) ----- S10

Summary of the sensing demonstration of PQT-12 OFETs (Table S3) ----- S11

**Section S1.** Procedures for self-assembled monolayer (SAM) treatment.

Before the surface treatment of SiO<sub>2</sub>/Si, the substrates were cleaned with Piranha solution (3:1 H<sub>2</sub>SO<sub>4</sub>:H<sub>2</sub>O<sub>2</sub>) and rinsed with toluene, acetone and isopropyl alcohol (IPA) sequentially and dried with nitrogen to obtain ultra-hydrophilic surface. The OTS solution for SAM treatment was prepared with *n*-octadecyltrimethoxysilane (OTS) and trichloroethylene (TCE) with the ratio of 12 μL and 10 mL respectively and stirred about 30 min. Then, the piranha-cleaned SiO<sub>2</sub>/Si substrate was spin-coated with the OTS solution with 1500 rpm for 30 s. After spincoating, the substrates were exposed to ammonium hydroxide (NH<sub>4</sub>OH) vapor under a pressure of about 10 ~ 50 mTorr for 12 h. Finally, the substrates were rinsed with toluene, acetone and IPA sequentially and dried with nitrogen stream. The contact angle of DI water on the OTS-modified wafer was approximately 109°.

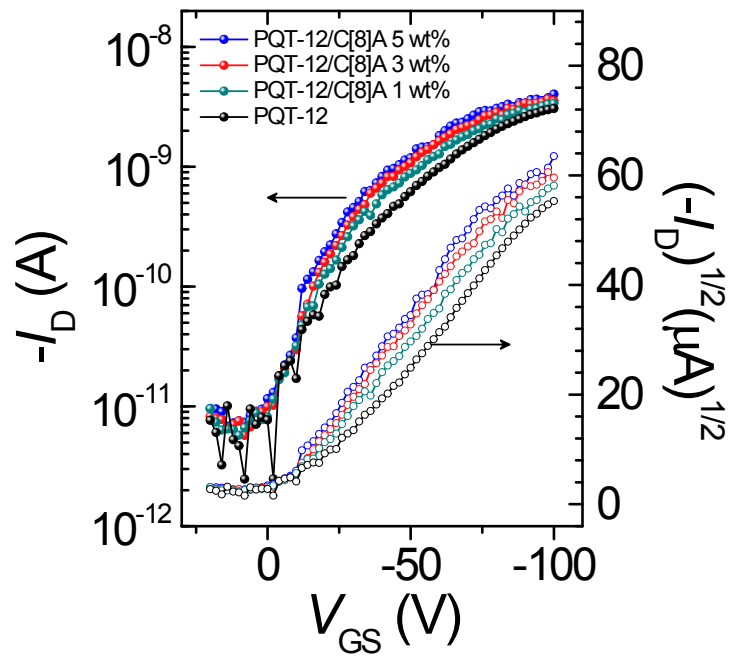


**Fig. S1** Transfer characteristics of PQT-12/C[8]A OFETs depending on the concentration of C[8]A. ( $V_{DS} = -100$  V).

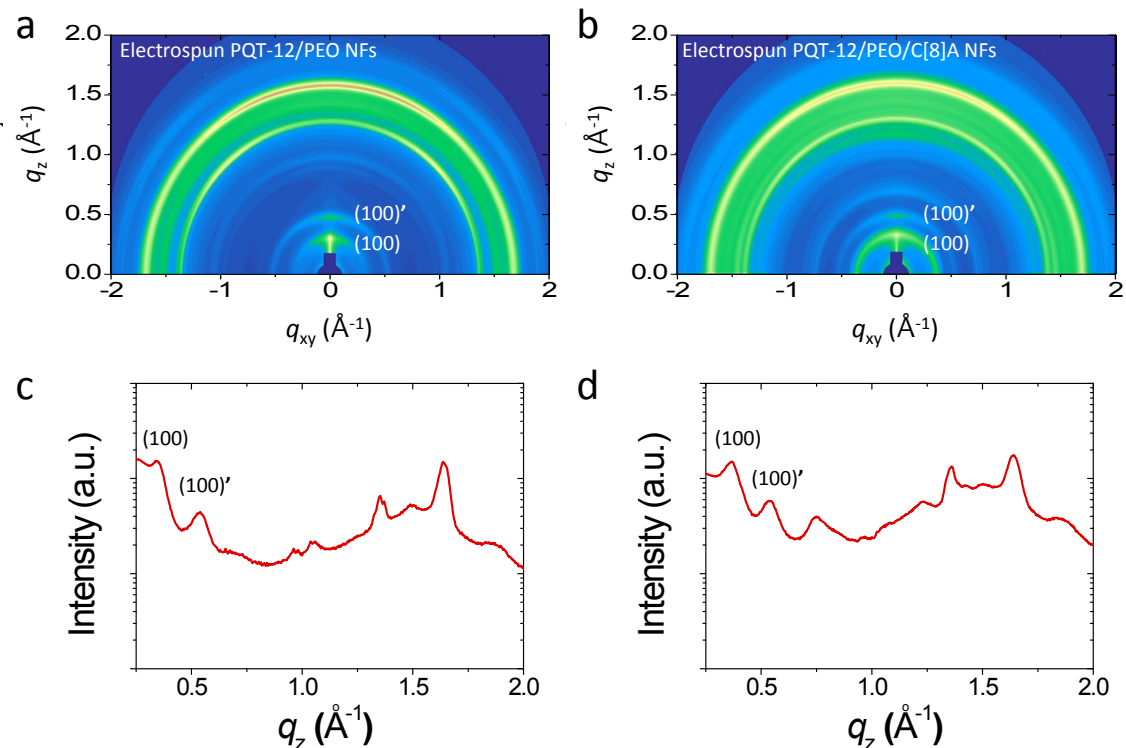


**Fig. S2** 2D-GIXD images of (a) PQT-12/PEO NFs and (b) PQT-12/PEO/C[8]A NFs of PQT-12:PEO (2:1, w/w). The corresponding GIXD diffractogram profiles; out-of-plane GIXD patterns of (c) PQT-12/PEO NFs and (d) PQT-12/PEO/C[8]A NFs. The higher order peaks of electrospun NFs of PQT-12:PEO were not easy to assign because of the lack of the information on the polymorphs of the electrospun NFs of the binary mixture.

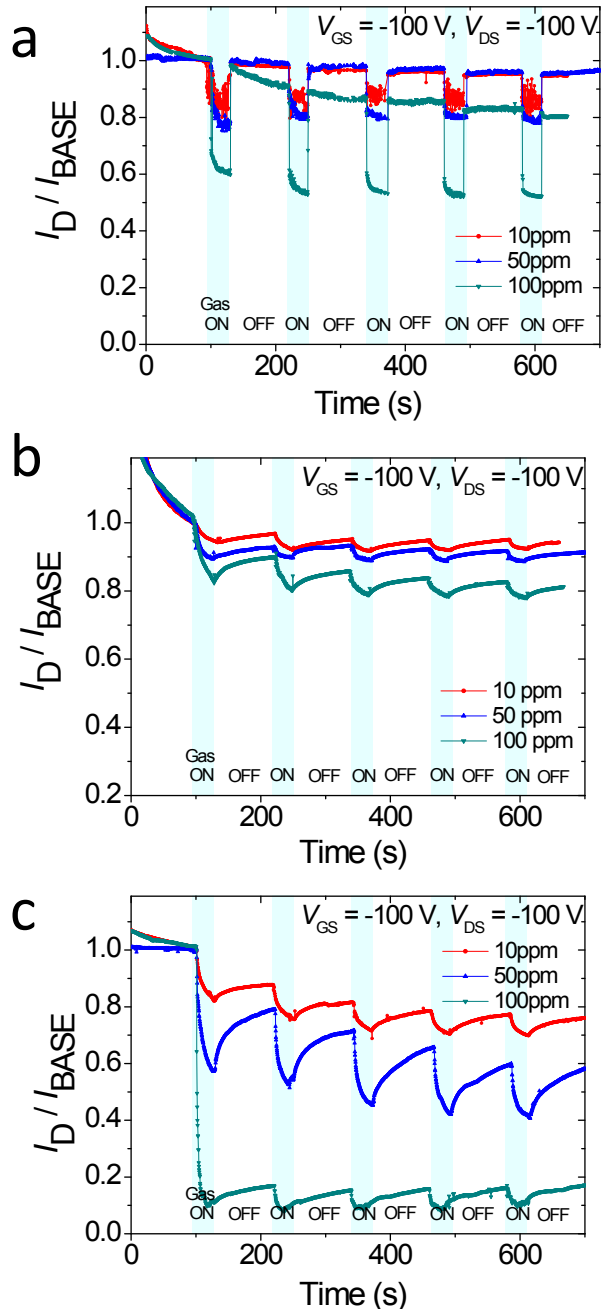


**Fig. S3** The normalized current change ( $I_D/I_{\text{BASE}}$ ) of a PQT-12/C[8]A OFET sensor is shown in response to periodic exposures to (a) ethanol, (b) n-hexane, and (c) toluene vapors at different concentrations.

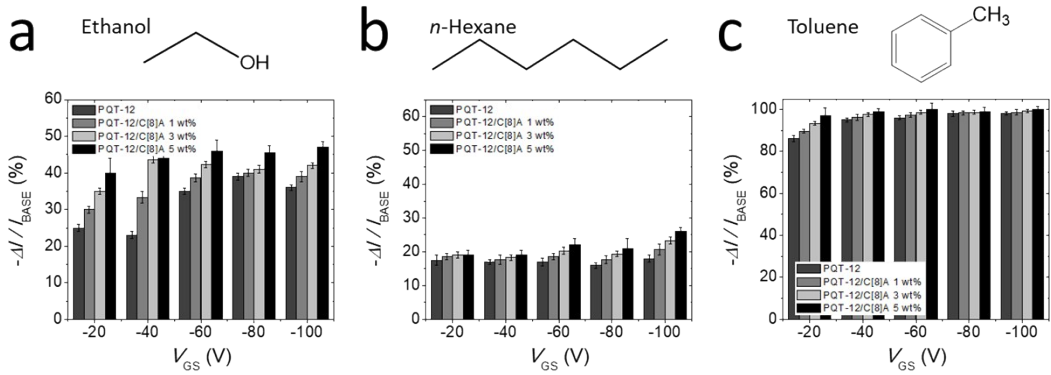


**Fig. S4** The relative responses of PQT-12 based OFET sensors are shown upon exposure to harsh conditions of VOCs ( $\approx 1000$  ppm) (a) ethanol, (b) *n*-hexane, and (c) toluene vapor. The bar values in y-axis indicate the normalized current change of PQT-12 and PQT-12/C[8]A OFET sensors as a function of  $V_{GS}$ , respectively.

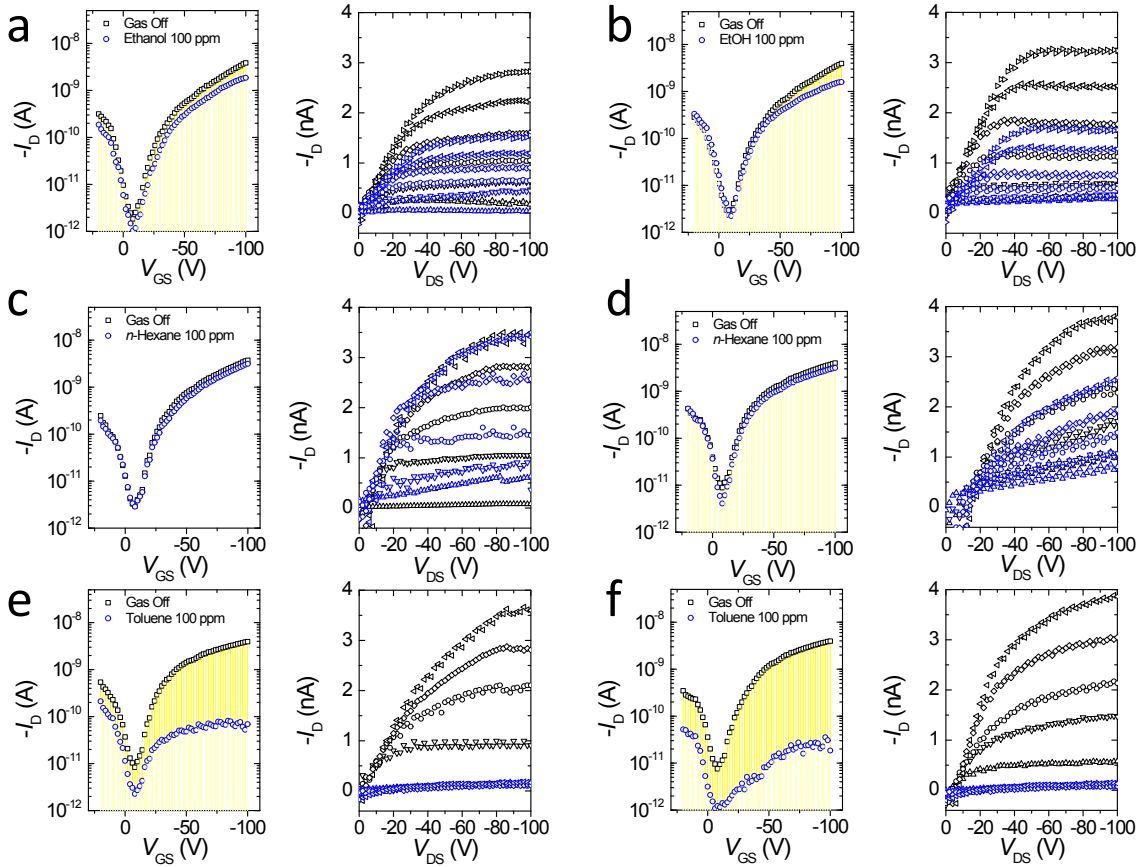


**Fig. S5** The transfer and output characteristics of (a, c, and e) PQT-12 NF and (b, d, and f) PQT-12/C[8]A OFET sensors was measured by electronic measurement equipment. Electrical characteristics were observed upon periodic exposure to (a and b) ethanol, (c and d) hexane, and (e and f) toluene vapor with 100 ppm different concentrations. Yellow drop lines emphasize the differences of  $I_D$  between PQT-12 NF and PQT-12/C[8]A OFET sensors.

**Table S1** Summary of the electrical characteristics of PQT-12/C[8]A NF based OFETs.

Condition	$\mu_h^{avg}$ [cm <sup>2</sup> V <sup>-1</sup> s <sup>-1</sup> ]	$\mu_h^{max}$ [cm <sup>2</sup> V <sup>-1</sup> s <sup>-1</sup> ]	$I_{on}/I_{off}$	$V_{TH}$ [V]
PQT-12	$3.2 \times 10^{-2}$	$5.1 \times 10^{-2}$	$1.1 \times 10^3$	0.8
PQT-12/C[8]A 1 wt%	$3.3 \times 10^{-2}$	$5.1 \times 10^{-2}$	$1.0 \times 10^3$	1.8
PQT-12/C[8]A 3 wt%	$3.7 \times 10^{-2}$	$5.7 \times 10^{-2}$	$1.4 \times 10^3$	2.1
PQT-12/C[8]A 5 wt%	$4.3 \times 10^{-2}$	$7.1 \times 10^{-2}$	$1.7 \times 10^3$	3.9

**Table S2** Primary lamellar spacing values of the two polymorphs of PQT-12 NFs and PQT-12/C[8]A NFs.

<b>Crystallographic parameters</b>	Electrospun PQT-12 NFs		Electrospun PQT-12/C[8]A NFs	
	(100)	(100)'	(100)	(100)'
From $q_z$ profile	$q \text{ [\AA}^{-1}]$	0.342	0.534	0.361
	$d\text{-spacing [\AA}^{-1}]$	18.38	11.76	17.41
				11.74

**Table S3** Summary of the sensing performance of PQT-12 and PQT-12/C[8]A 5 wt% OFET for VOCs of 100 ppm. The  $dI_D$  indicates the differences of  $I_D$  value of the sensors exposed to VOCs from that without exposure to VOCs.

$V_{GS}$ [V]	Ethanol		<i>n</i> -Hexane		Toluene	
	$dI_D$ (w/o) [A]	$dI_D$ (C[8]A) [A]	$dI_D$ (w/o) [A]	$dI_D$ (C[8]A) [A]	$dI_D$ (w/o) [A]	$dI_D$ (C[8]A) [A]
-20	$1.30 \times 10^{-11}$	$7.74 \times 10^{-11}$	$6.82 \times 10^{-12}$	$1.57 \times 10^{-11}$	$3.10 \times 10^{-11}$	$5.56 \times 10^{-11}$
-40	$1.49 \times 10^{-10}$	$2.94 \times 10^{-10}$	$1.09 \times 10^{-10}$	$1.33 \times 10^{-10}$	$2.48 \times 10^{-10}$	$6.33 \times 10^{-10}$
-60	$3.90 \times 10^{-10}$	$6.19 \times 10^{-10}$	$2.49 \times 10^{-10}$	$2.77 \times 10^{-10}$	$3.54 \times 10^{-10}$	$1.68 \times 10^{-9}$
-80	$8.03 \times 10^{-10}$	$2.80 \times 10^{-9}$	$3.67 \times 10^{-10}$	$5.24 \times 10^{-10}$	$5.79 \times 10^{-10}$	$2.82 \times 10^{-9}$
-100	$1.39 \times 10^{-9}$	$1.99 \times 10^{-9}$	$5.94 \times 10^{-10}$	$8.50 \times 10^{-10}$	$8.48 \times 10^{-10}$	$3.94 \times 10^{-9}$